Prediction and Retrodiction for a Continuously Monitored Superconducting Qubit

D. Tan, S. J. Weber, I. Siddiqi, K. Mølmer, and K. W. Murch

Phys. Rev. Lett. **114**, 090403 — Published 5 March 2015

DOI: 10.1103/PhysRevLett.114.090403

Prediction and retrodiction for a continuously monitored superconducting qubit

D. Tan,[1] S. J. Weber,[2] I. Siddiqi,[2] K. Mølmer,[3] and K. W. Murch*[1]

[1]*Department of Physics, Washington University, St. Louis, Missouri 63130*
[2]*Quantum Nanoelectronics Laboratory, Department of Physics, University of California, Berkeley CA 94720*
[3]*Department of Physics and Astronomy, Aarhus University, Ny Munkegade 120, DK-8000 Aarhus C, Denmark*

(Dated: February 13, 2015)

The quantum state of a superconducting transmon qubit inside a three-dimensional cavity is monitored by transmission of a microwave field through the cavity. The information inferred from the measurement record is incorporated in a density matrix ρ_t, which is conditioned on probe results until t, and in an auxiliary matrix E_t, which is conditioned on probe results obtained after t. Here, we obtain these matrices from experimental data and we illustrate their application to predict and retrodict the outcome of weak and strong qubit measurements.

In quantum mechanics, predictions about the outcome of experiments are given by Born's rule which for a state vector $|\psi_i\rangle$ provides the probability $P(a) = |\langle a|\psi_i\rangle|^2$ that a measurement of an observable $\hat{A}$ with eigenstates $|a\rangle$ yields one of the eigenvalues a. As a consequence of the measurement, the quantum state is projected into the state $|a\rangle$. Yet, after this measurement, further probing of the system is possible, and the probability that the quantum system yields outcome a and is subsequently detected in a final state $|\psi_f\rangle$ factors into the product $|\langle\psi_f|a\rangle|^2|\langle a|\psi_i\rangle|^2$. Considering initial and final states raises the issue of post-selection in quantum measurements: What is the probability that the result of the measurement of $\hat{A}$ *was* a, if we consider only the selected measurement events where the initial state was $|\psi_i\rangle$ and the final state was $|\psi_f\rangle$? The answer is known as the Aharonov-Bergmann-Lebowitz rule [1],

$$P_{ABL}(a) = \frac{P(f,a|i)}{\sum_{a'} P(f,a'|i)} = \frac{|\langle\psi_f|a\rangle\langle a|\psi_i\rangle|^2}{\sum_{a'}|\langle\psi_f|a'\rangle\langle a'|\psi_i\rangle|^2} \quad (1)$$

and it differs from Born's rule, which takes into account only knowledge about the state prior to the measurement.

While it is natural that full measurement records reveal more information about the state of a physical system at a given time t than data obtained only until that time, the interpretation of the time symmetric influences from the future and from the past measurement events on P_{ABL} has stimulated some debate, see for example [1–6]. Meanwhile, probabilistic state assignments and correlations observed in atomic, optical and solid state experiments have been conveniently understood in relation to post-selection [7–11], and precision probing theories [12–17] have incorporated full measurement records.

In this letter, we consider a superconducting qubit that is subject to continuous monitoring and driven unitary evolution. We apply a recent generalization [18] of Eq.(1) to the case of continuously monitored and evolving mixed states. This incorporates continuous measurement outcomes before *and* after t to retrodict the probabilities for arbitrary measurements performed at time t. Our experiments verify the probabilities assigned to projective measurements and the mean values assigned to weak (weak value) measurements which are both nontrivially different from predictions based only on the measurement record up to time t.

To analyze non-pure states and partial measurements, we represent our system by a density matrix ρ, and measurements by the theory of positive operator-valued measures (POVM) which yields the probability $P(m) = \mathrm{Tr}(\Omega_m\rho\Omega_m^\dagger)$ for outcome m, and the associated back action on the quantum state, $\rho \to \Omega_m\rho\Omega_m^\dagger/P(m)$, where the operators Ω_m obey $\sum_m \Omega_m^\dagger\Omega_m = \hat{I}$. When $\Omega_a = |a\rangle\langle a|$ is a projection operator and $\rho = |\psi\rangle\langle\psi|$, the theory of POVMs is in agreement with Born's rule.

For systems subject to unitary and dissipative time evolution along with continuous monitoring before and after a measurement described by operator Ω_m, one can show [18] that,

$$P_p(m) = \frac{\mathrm{Tr}(\Omega_m\rho_t\Omega_m^\dagger E_t)}{\sum_m \mathrm{Tr}(\Omega_m\rho_t\Omega_m^\dagger E_t)}, \quad (2)$$

where ρ_t is the system density matrix at time t, conditioned on previous measurement outcomes, and propagated forward in time until time t, while E_t is a matrix which is propagated backwards in time in a similar manner and accounts for the time evolution and measurements obtained after time t. The subscript $\cdot_p$ denotes "past", and in [18] it was proposed that, if t is in the past, the pair of matrices (ρ_t, E_t), rather than only ρ_t, is the appropriate object to associate with the state of a quantum system at time t. We observe that for the case of pure states and projective measurements, $P_p(m)$ in (2) acquires the form of Eq.(1) with $\rho_t = |\psi_i\rangle\langle\psi_i|$ and $E_t = |\psi_f\rangle\langle\psi_f|$.

Here, we make use of the full measurement record to compute the matrices ρ_t and E_t, and analyze how they, through application of Eq.(2) yield different predictions for measurements on the system. For imperfect measurement efficiency, non-pure states, and measurements that do not commute with the system evolution, the predic-

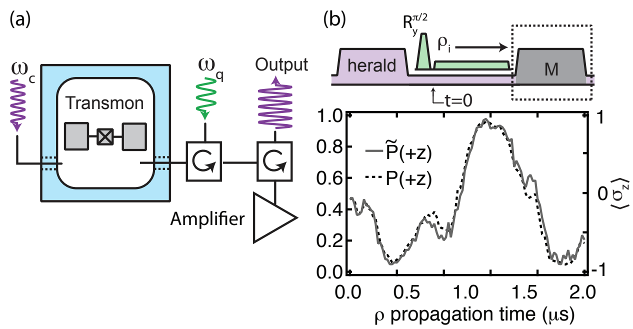

Figure 1: Time evolution in a monitored system. (a) Simplified experimental setup consisting of a transmon circuit coupled to a waveguide cavity. (b) We prepare the qubit in an initial state ($\mathrm{Tr}(\rho_i\sigma_x) \simeq +1$) and propagate ρ forward in time, which makes accurate predictions about a final projective measurement (in the σ_z basis) labeled M. The dashed line is the prediction based on a single quantum trajectory, and the solid line is the result from projective measurements on an ensemble of experiments that have similar values of ρ_t.

tions of Eq.(2) vary dramatically from those based on ρ alone [20, 21].

Our experiment, illustrated in figure 1a, is composed of a superconducting transmon circuit dispersively coupled to a wave-guide cavity [22, 23]. The two lowest energy levels of the transmon form a qubit with transition frequency $\omega_q/2\pi = 4.0033$ GHz. The dispersive coupling between the transmon qubit and the cavity is given by an interaction Hamiltonian, $H_{\mathrm{int.}} = -\hbar\chi a^\dagger a\sigma_z$, where $\hbar$ is the reduced Plank's constant, $a^\dagger(a)$ is the creation (annihilation) operator for the cavity mode at frequency $\omega_c/2\pi = 6.9914$ GHz, $\chi/2\pi = -0.425$ MHz is the dispersive coupling rate, and σ_z is the qubit Pauli operator that acts on the qubit in the energy basis. A microwave tone that probes the cavity with an average intracavity photon number $\bar{n} = \langle a^\dagger a\rangle$ thus acquires a qubit-state-dependent phase shift. Since $2|\chi| \ll \kappa$, where $\kappa/2\pi = 9.88$ MHz is the cavity linewidth, qubit state information is encoded in one quadrature of the microwave signal. We amplify this quadrature of the signal with a near-quantum-limited Josephson parametric amplifier [24]. After further amplification, the measurement signal is demodulated and digitized. This setup allows variable strength measurements of the qubit state characterized by a measurement timescale τ; by binning the measurement signal in time steps $\delta t \ll \tau$ we execute weak measurements of the qubit state [20, 25] while by integrating the measurement signal for a time $T \gg \tau$ we effectively accumulate weak measurements in a projective measurement [26] of the qubit in the σ_z basis.

Our experimental sequences begin with a projective measurement of the qubit in the σ_z basis followed by a variable rotation of the qubit state to prepare the qubit in an arbitrarily specified initial (nearly) pure state. Following this preparation, the qubit is subject to continuous rotations given by $H_{\mathrm{R}} = \hbar\Omega_R\sigma_y/2$, where $\Omega_R/2\pi = 0.7$ MHz is the Rabi frequency, and continuous probing given by the measurement operator $\sqrt{k}\sigma_z$, where $k = 4\chi^2\bar{n}/\kappa = 1/4\eta\tau$ parametrizes the measurement strength ($k/2\pi = 95$ kHz) and $\eta = 0.35$ is the quantum measurement efficiency [27]. During probing, we digitize the measurement signal V_t in time steps $\delta t = 20$ ns.

The density matrix associated with a given measurement signal V_t is obtained by solving the stochastic master equation [19]:

$$\begin{aligned}\frac{d\rho}{dt} = &-\frac{\mathbf{i}}{\hbar}[H_{\mathrm{R}}, \rho] + k(\sigma_z\rho\sigma_z - \rho)\\ &+ 2\eta k(\sigma_z\rho + \rho\sigma_z - 2\mathrm{Tr}(\sigma_z\rho)\rho)V_t. \quad (3)\end{aligned}$$

Here, the first two terms are the standard master equation in Lindblad form, and the last stochastic term updates the state based on the measurement result and leads to quantum trajectory solutions that are different for every repetition of the experiment.

Let us first recall how the density matrix makes predictions about the outcome of measurements. In figure 1b, we consider the probabilities $P(\pm z)$ for the outcome of the projective measurement operators $\Omega_{\pm z} = (\sigma_z \pm 1)/2$. We prepare the initial state, $\mathrm{Tr}(\rho_i\sigma_x) \simeq +1$, by heralding the ground state and applying a $\pi/2$ rotation about the y axis. We then propagate ρ_t forward from this initial state, and at each point in time we display the calculated $P(+z) = \mathrm{Tr}(\Omega_{+z}\rho_t\Omega_{+z}^\dagger)$ [27]. By performing projective measurements of $\Omega_{\pm z}$ at time t on an ensemble of experiments that have similar values of ρ_t (within ± 0.02) we obtain the corresponding experimental result $\tilde{P}(+z)$. We perform this analysis at different times and we observe close agreement between the single quantum trajectory prediction $P(+z)$ and the observed $\tilde{P}(+z)$. Note that the same procedure was used to tomographically reconstruct and verify the quantum trajectory associated with the mean value $\langle\sigma_z\rangle = 2P(+z) - 1$ in [20, 21].

We now turn to the application of measurement data to retrodict the outcome of an already performed measurement. Eq.(2) applies for any set of POVM measurement operators Ω_m at time t, and accumulates the information retrieved from the later probing in the matrix E_t that is propagated *backwards* in time according to [18],

$$\begin{aligned}\frac{dE}{dt} = &\frac{\mathbf{i}}{\hbar}[H_{\mathrm{R}}, E] + k(\sigma_z E\sigma_z - E)\\ &+ 2\eta k(\sigma_z E + E\sigma_z - 2\mathrm{Tr}(\sigma_z E)E)V_{t-dt}. \quad (4)\end{aligned}$$

We assume that no measurements take place beyond the time T, leading to the final condition $E_T = \hat{I}/2$ [18]. If no measurements take place at all before T, for example because $\eta = 0$, Eq.(4) yields a solution for $E(t)$ that remains proportional to the identity operator for all

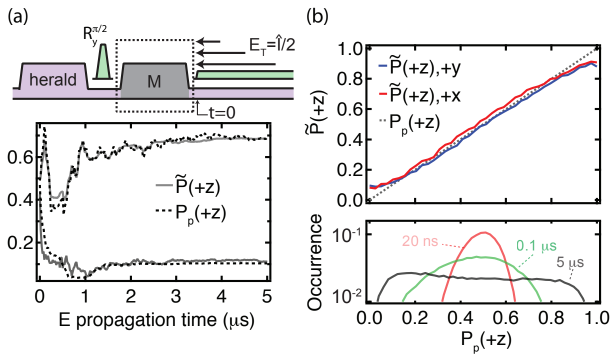

Figure 2: Retrodiction in a monitored system. (a) To test retrodictions made by E we prepare different states ρ_i and conduct a subsequent projective measurement M. We propagate E backwards from the final state $E_T = \hat{I}/2$ to E_0 for variable periods of time (T). This yields a retrodiction (shown as dashed lines for two different experiments) for the outcome of M. The solid line, which is based on an ensemble of experiments that yielded similar values of E_0 confirms the retrodictions based on the single measurement record. (b) We prepare two different initial states ($\mathrm{Tr}(\rho_i\sigma_x) \simeq +1$, red, $\mathrm{Tr}(\rho_i\sigma_y) \simeq +1$, blue), and compare the retrodictions, $P_p(+z)$, based on 5 μs of probing, to the outcomes of measurements M that yielded similar values of E_0. In the lower panel, we display histograms of $P_p(+z)$ for different propagation times. As more of the record is included, the retrodicted probabilities assume a wider range of values.

times, and Eq.(2) leads to the conventional expression that depends only on ρ_t.

In figure 2 we test the retrodictions made by E and Eq.(2). We examine different initial states, $\mathrm{Tr}(\rho_i\sigma_x) \simeq +1$, $\mathrm{Tr}(\rho_i\sigma_y) \simeq +1$, which are prepared by heralding the ground state and applying $\pi/2$ rotations about the y and $-x$ axes respectively. We propagate E backwards from E_T to E_0 to make a retrodiction about a projective measurement M. Note that while the initial states ρ_i make ambiguous predictions about the outcome of M, $P(+z) = 1/2$, the retrodiction for the outcome of M becomes biased by the information obtained later and incorporated in the matrix E.

We verify that the retrodictions are correct by averaging the outcomes of many measurements M that corresponded to similar values of E_0 to obtain an experimentally derived probability, $\tilde{P}(+z)$. Figure 2a displays two sample trajectories for the retrodiction $P_p(+z)$ along with $\tilde{P}(+z)$. As more information is included, the retrodictions converge to fixed values. Figure 2b displays the results of 3×10^5 experimental tests for the two different initial states ρ_i. For both initial states and for a wide range of measurement outcomes we are able to tomographically verify the retrodictions. We also display histograms of the different values $P_p(+z)$ for different propagation times of E. The larger the bias of $P_p(+z)$ compared to $P(+z)$, the more often our hindsight enables a correct guess of the outcome of the projective σ_z measurement.

Having verified the predictions based on ρ, and the retrodictions based on E, we now aim to illustrate the application of ρ and E to use both past and future information to predict the outcome of a POVM measurement. The POVM measurement that we consider is simply a short segment of the measurement signal received between t and $t + \Delta t$ and is given by the measurement operators [19, 28],

$$\Omega_V = \left(2\pi a^2\right)^{-1/4} e^{(-(V-\sigma_z)^2/4a^2)} \tag{5}$$

where, $1/4a^2 = k\eta\Delta t$. The operators Ω_V satisfy $\int \Omega_V^\dagger \Omega_V dV = \hat{I}$ as expected for POVMs, and if we assume that ρ_t can be treated as a constant during Δt, the probability of the measurement yielding a value V is $P(V) = \mathrm{Tr}(\Omega_V \rho_t \Omega_V^\dagger)$, which is the sum of two Gaussian distributions with variance a^2 centered at $+1$ and -1 and weighted by the populations ρ_{00} and ρ_{11} of the two qubit states. The σ_z term in Ω_V causes the back action on the qubit degree of freedom, $\rho \rightarrow \Omega_V \rho \Omega_V^\dagger$, due to the readout of the measurement result V. If the effects of damping and the Rabi drive can be ignored during Δt, the operators (5) also describe a stronger measurement, yielding ultimately the limit where the two Gaussian distributions are disjoint, and the readout causes projective back action of the qubit on one of its σ_z eigenstates, with probabilities ρ_{00} and ρ_{11}.

Since the system is also subject to probing and evolution after t, we now examine what hindsight predictions can be made for the outcome of the measurement Ω_V based on both earlier *and* later probing. We must hence evaluate the conditioned density matrix ρ_t and the matrix E_t and Eq.(2) yields the outcome probability distribution expressed in terms of their matrix elements,

$$\begin{aligned} P_p(V) \propto & \rho_{00}E_{00}e^{(-(V-1)^2/2a^2)} + \rho_{11}E_{11}e^{(-(V+1)^2/2a^2)} \\ & + (\rho_{10}E_{01} + \rho_{01}E_{10})e^{(-(V^2+1)/2a^2)}. \end{aligned}$$

We observe that the information obtained after the measurement of interest plays a formally equally important role as the conditional quantum state represented by ρ.

The predicted mean value is $\langle V \rangle_p = \int P_p(V) V dV$, and can be evaluated,

$$\langle V \rangle_p = \frac{(\rho_{00}E_{00} - \rho_{11}E_{11})}{(\rho_{00}E_{00} + \rho_{11}E_{11} + \exp(-\frac{1}{8a^2})(\rho_{10}E_{01} + \rho_{01}E_{10})}. \tag{6}$$

Here we note that if the measurement is strong, a is small, and the coherence contribution is cancelled in the denominator, yet if the measurement is weak, a single measurement is dominated by noise and reveals only little information (and causes infinitesimal back action). This is the situation that leads to so-called weak values. If the

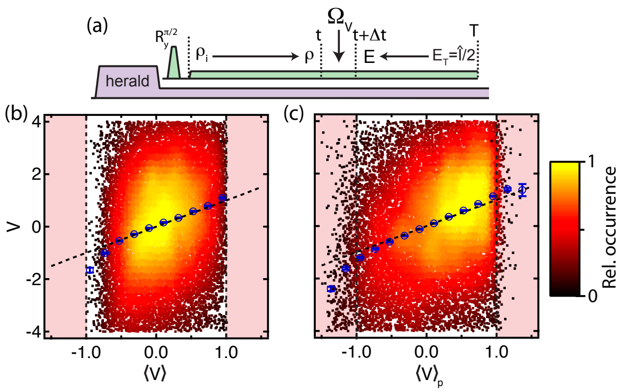

Figure 3: Conventional and past quantum state predictions for the measurement Ω_V conducted at time t. (a) The experiment sequence initializes the qubit along $+x$ and probes the cavity while the qubit transition is driven with a constant Rabi frequency. Each experiment yields a value V resulting from the Ω_V measurement and predicted mean values $\langle V\rangle$ (which is based on ρ), and $\langle V\rangle_p$ (which is based on ρ and E). We plot V versus $\langle V\rangle$ (b), and $\langle V\rangle_p$ (c) and find that the conditional average of V (open circles) is in agreement with the expected mean value given by the dashed line. Note that $\langle V\rangle_p$ makes predictions for the mean value that fall outside of the spectral range of the qubit observable (in the pink region).

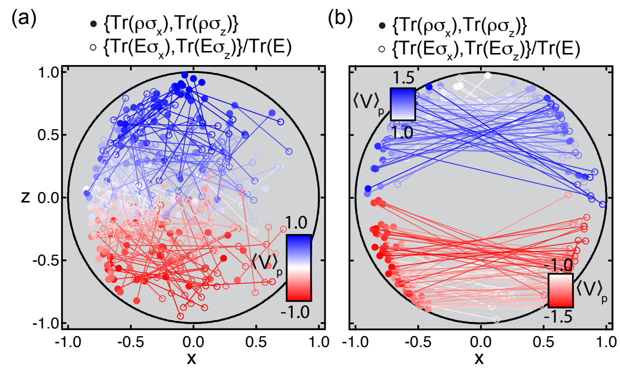

Figure 4: Bloch vector representation of the matrix elements of ρ and E. For each iteration of the experiment, a line joins the coordinates $\{\mathrm{Tr}(\rho\sigma_x), \mathrm{Tr}(\rho\sigma_z)\} = \{\langle\sigma_x\rangle, \langle\sigma_z\rangle\}$ (closed circles) and $\frac{1}{\mathrm{Tr}(E)}\{\mathrm{Tr}(E\sigma_x), \mathrm{Tr}(E\sigma_z)\}$ (open circles). The closed circles represents the state of the system at time t based on ρ_t, and the open circles represent the corresponding quantity based on $E_{t+\Delta t}$. The color indicates the value of $\langle V\rangle_p$ for each pair of states. Panel (a) displays some of the the matrix elements that yield normal predictions ($|\langle V\rangle_p| \le 1$), and panel (b) displays a sample of matrix elements that yield anomalous ($|\langle V\rangle_p| > 1$) predictions.

measurement signal is proportional to an observable $\hat{A}$, and the system is initialized in $|\psi_i\rangle$ and post-selected in state $|\psi_f\rangle$, the mean signal is given by [29],

$$\langle \hat{A}_w\rangle = Re[\frac{\langle\psi_f|\hat{A}|\psi_i\rangle}{\langle\psi_f|\psi_i\rangle}], \tag{7}$$

which may differ dramatically from the usual expectation value $\langle\psi_i|\hat{A}|\psi_i\rangle$. Our Eq.(2) has, indeed, been derived by Wiseman [30] to clarify how weak values are related to continuous quantum trajectories and correlations in field measurements.

In figure 3, we display results of our experiments that test the predictions of Eq.(6). For many iterations of the experiment we choose a measurement time interval, $\Delta t = 180$ ns that is short enough that the effect of the continuous Rabi drive is nearly negligible in the time interval $(t, t+\Delta t)$. Based on 800 ns of probing before t, we calculate $P(V)$, and based on 800 ns of probing before *and* after the measurement interval, we calculate $P_p(V)$ for the result of the measurement. In Fig. 3, we show that both the conventional and the past quantum state formalism yield agreement between the predicted mean value and the measured values. The measured results are noisy, and we plot the data with the predicted average value along the horizontal axes, and the measured values along the vertical axes.

While $\langle V\rangle = \langle\sigma_z\rangle$, and thus never exceeds 1, a fraction of the experiments lead to prediction and observation of values $|\langle V\rangle_p| > 1$. Such anomalous weak walues in connection with Eq.(7) have been typically identified with the intentional post selection of final states with a very small overlap with the initial state. Surprisingly, continuous probing leads to similar effects [21]. In figure 4 we examine the states that lead to different weak value predictions. We represent pairs of ρ and E as connected points on the Bloch sphere. Indeed, predictions outside the spectral range of the operator are accompanied by near orthogonality of states associated with the matrices ρ_t and $E_{t+\Delta t}$. In agreement with the pure state case, large weak values of σ_z do not occur when ρ_t or $E_{t+\Delta t}$ are close to the σ_z eigenstates, but rather when they are close to opposite σ_x eigenstates.

In conclusion, we have demonstrated the use of the quantum trajectory formalism to infer the quantum state of a superconducting qubit conditioned on the outcome of continuous measurement. We have also demonstrated a quantum hindsight effect, where probing of a quantum system modifies and improves the predictions about measurements already performed in the past. These advances may be used to improve the state preparation and readout fidelity for quantum systems and increase their potential for use as probes [12–17] of time-dependent interactions and parameter estimation.

*murch@physics.wustl.edu

[1] Y. Aharonov, P. G. Bergmann, and J. L. Lebowitz, Phys. Rev. **134**, B1410 (1964).
[2] S. Watanabe, Rev. Mod. Phys. **27**, 179 (1955).
[3] Y. Aharonov, S. Popescu, and J. Tollaksen, Physics Today **63**, 27 (2010).
[4] Y. Aharonov, S. Popescu, and J. Tollaksen, Physics Today **64**, 62 (2011).
[5] Y. Aharonov, S. Popescu, and J. Tollaksen, Physics Today **64**, 9 (2011).
[6] L. Vaidman, Phys. Rev. A **87**, 052104 (2013).
[7] S. Gammelmark, K. Mølmer, W. Alt, T. Kampschulte, and D. Meschede, Phys. Rev. A **89**, 043839 (2014).
[8] M. E. Goggin, M. P. Almeida, M. Barbieri, B. P. Lanyon, J. L. OÕBrien, A. G. White, and G. J. Pryde, Proc. Natl. Acad. Sci. U.S.A. **108**, 1256 (2011).
[9] G. Waldherr, P. Neumann, S. F. Huelga, F. Jelezko, and J. Wrachtrup, Phys. Rev. Lett. **107**, 090401 (2011).
[10] J. P. Groen, D. Ristè, L. Tornberg, J. Cramer, P. C. de Groot, T. Picot, G. Johansson, and L. DiCarlo, Phys. Rev. Lett. **111**, 090506 (2013).
[11] P. Campagne-Ibarcq, L. Bretheau, E. Flurin, A. Auffèves, F. Mallet, and B. Huard, Phys. Rev. Lett. **112**, 180402 (2014).
[12] M. Tsang, Phys. Rev. Lett. **102**, 250403 (2009).
[13] M. Tsang, Phys. Rev. A **80**, 033840 (2009).
[14] M. Tsang, H. M. Wiseman, and C. M. Caves, Phys. Rev. Lett. **106**, 090401 (2011).
[15] M. A. Armen, A. E. Miller, and H. Mabuchi, Phys. Rev. Lett. **103**, 173601 (2009).
[16] T. A. Wheatley, D. W. Berry, H. Yonezawa, D. Nakane, H. Arao, D. T. Pope, T. C. Ralph, H. M. Wiseman, A. Furusawa, and E. H. Huntington, Phys. Rev. Lett. **104**, 093601 (2010).
[17] T. Rybarczyk, S. Gerlich, B. Peaudecerf, M. Penasa, B. Julsgaard, K. M. lmer, S. Gleyzes, M. Brune, J.-M. Raimond, S. Haroche, et al., arXiv p. 1409.0958 (2014).
[18] S. Gammelmark, B. Julsgaard, and K. Mølmer, Phys. Rev. Lett. **111**, 160401 (2013).
[19] H. Wiseman and G. Milburn, *Quantum Measurement and Control* (Cambridge University Press, 2010).
[20] K. W. Murch, S. J. Weber, C. Macklin, and I. Siddiqi, Nature **502**, 211 (2013).
[21] S. J. Weber, A. Chantasri, J. Dressel, A. N. Jordan, K. W. Murch, and I. Siddiqi, Nature **511**, 570Ð573 (2014).
[22] J. Koch, T. M. Yu, J. Gambetta, A. A. Houck, D. I. Schuster, J. Majer, A. Blais, M. H. Devoret, S. M. Girvin, and R. J. Schoelkopf, Phys. Rev. A **76**, 042319 (2007).
[23] H. Paik, D. I. Schuster, L. S. Bishop, G. Kirchmair, G. Catelani, A. P. Sears, B. R. Johnson, M. J. Reagor, L. Frunzio, L. I. Glazman, et al., Phys. Rev. Lett. **107**, 240501 (2011).
[24] M. Hatridge, R. Vijay, D. H. Slichter, J. Clarke, and I. Siddiqi, Phys. Rev. B **83**, 134501 (2011).
[25] M. Hatridge, S. Shankar, M. Mirrahimi, F. Schackert, K. Geerlings, T. Brecht, K. M. Sliwa, B. Abdo, L. Frunzio, S. M. Girvin, et al., Science **339**, 178 (2013).
[26] R. Vijay, D. H. Slichter, and I. Siddiqi, Phys. Rev. Lett. **106**, 110502 (2011).
[27] Further details regarding the propagation of ρ and E, the experimental setup, and data analysis are given in supplemental information.
[28] K. Jacobs and D. A. Steck, Contemp. Phys. **47**, 279 (2006).
[29] Y. Aharonov, D. Z. Albert, and L. Vaidman, Phys. Rev. Lett. **60**, 1351 (1988).
[30] H. M. Wiseman, Phys. Rev. A **65**, 032111 (2002).